Contribution from the Department of Chemistry,
University of Western Ontario, London, Ontario, N6A 5B7 Canada

Photochemical, Electrochemical, and Chemical Formation of the π-Cation-Radical Species of Magnesium Phthalocyanine. Analysis of the Absorption and MCD Spectra of $[MgPc(-1)]^{\bullet+}$

Edward Ough, Zbigniew Gasyna, and Martin J. Stillman*

Received July 26, 1990

Photochemical, electrochemical, and chemical methods have been used to form the ring-oxidized, π-cation-radical species of magnesium phthalocyanine, $[MgPc(-1)]^{\bullet+}$. Photooxidation of MgPc(-2) was carried out by excitation with visible region light into the phthalocyanine Q band at 670 nm, using carbon tetrabromide as an irreversible electron acceptor. The radical cation was also formed by controlled potential coulometry at the first oxidation potential (+0.70 V vs SCE) of MgPc(-2) and by chemical oxidation with nitric acid. Absorption and magnetic circular dichroism (MCD) spectra are reported between 250 and 850 nm for $[(L)_nMgPc(-1)]^{\bullet+}$ (n = 1, 2) π-cation-radical species, where L = imidazole, 4-methylimidazole, pyridine, methylpyridine, or cyanide. The first low-temperature absorption and MCD spectra (at 200 K) of $[MgPc(-1)]^{\bullet+}$ are reported, under which conditions it is shown that the cation-radical species dimerizes completely. Electron paramagnetic resonance (EPR) spectra confirm that at low temperatures the unpaired spins couple. At elevated temperatures (>300 K) in dichloroethane, the monomer predominates. Band deconvolution calculations, which couple fits for both absorption and MCD spectra, are reported for each of the radical-cation species. These results are compared to previous band assignments and the deconvolution results for $[ZnPc(-1)]^{\bullet+}$ reported by Nyokong, Gasyna, and Stillman (*Inorg. Chem.* **1987**, *26*, 1087-1095). At room temperature, the spectra arise from a mixture of monomers and dimers. For $[(im)_nMgPc(-1)]^{\bullet+}$, nine well-resolved transitions are centered near 825 nm (12 100 cm^{-1}), 717 nm (13 900 cm^{-1}), 507 nm (19 700 cm^{-1}), 422 nm (23 700 cm^{-1}), 372 nm (26 900 cm^{-1}), 319 nm (31 300 cm^{-1}), 276 nm (36 300 cm^{-1}), 266 nm (37 700 cm^{-1}), and 255 nm (39 200 cm^{-1}). Major band maxima in the experimental spectral data of the monomer are located at 825, 505, 411, 387, and 328 nm. Major band maxima in the spectra of the dimer (measured at 200 K) are located at 712, 510, 370, 317, and 277 nm. Deconvolution of the absorption and MCD spectra indicate that all but the 507-nm absorption band arise from degenerate transitions. Calculations provide band centers at 826 (Q), 507, 413 (B1), 387 (B2), 330, 315, and 277 nm for the monomer and at 717 nm (Q), 507, 422 (B1), 372 (B2), 319, 276, and 255 nm for the dimer. The 507-nm band is assigned to a nondegenerate transition from a low-lying molecular orbitals into the half-filled $a_{1u}(\pi)$ molecular orbital. Analysis of these data identify transitions specifically related to the $^2A_{1u}$ ground state of the ring, allowing comparisons to be made with the spectral data from $[ZnTPP(-1)]^{\bullet+}$, a species with the $^2A_{2u}$ ground state.

Introduction

The chemistry of metallophthalocyanine (MPc(-2)) ring complexes has been well studied.[1] The phthalocyanines exhibit chemistry and spectroscopic properties that are distinct from those of the parent porphyrin. Interest in these complexes arises in part from their use as models for the heme proteins and chlorophylls[2-8] and in part from their extensive electrochemical properties that make them useful as catalysts, photochemical redox agents in solar energy conversion, visual pigments in displays, and photosensitizers for photodynamic therapy.[1,9-11] (We should note that the nomenclature for the charge on the ring gives Pc(-2) as the dianion, so that when complexed with a dicationic metal, the overall complex is neutral. For ring-oxidized cations, the ring charge is expressed as Pc(-1), Pc(0), etc. so that the overall charge is +1 for $[Mg(II)Pc(-1)]^{\bullet+}$.[1]

Studies of the electrochemical and photochemical properties of porphyrins are facilitated by their high solubility in a wide range of solvents; similar studies with phthalocyanines have been hindered by their limited solubility. An improvement in the solubility of phthalocyanines is achieved by attaching sulfate groups to the outer periphery of the fused benzene rings, but aggregation makes it difficult to fully interpret the resultant spectroscopic and electrochemical data.[12,13] Group 1 and group 2 metal-substituted phthalocyanines are very much more soluble in spectroscopically transparent and electrochemically useful solvents. Magnesium phthalocyanine exhibits no bands due to charge transfer between 200 and 1000 nm in its absorption spectrum.[4] Because MgPc(-2) is highly soluble in methylene chloride, formation of concentrated solutions of the radical cation by a variety of methods is also possible. Thus MgPc(-2) serves as an ideal model for the spectral properties of both neutral and oxidized phthalocyanines.

The two top filled molecular orbitals in metallophthalocyanines are assigned symmetry labels of a_{1u} and a_{2u}, with a_{1u} highest in energy.[1,5] Oxidation of phthalocyanines yields $^2A_{1u}$ as the ground state for the ring. Therefore, the $[MgPc(-1)]^{\bullet+}$ species models the extreme situation of the electronic arrangement in many complexes of octaethylporphyrin (OEP)[14,15] and in the heme enzyme catalase,[16] in which it is suggested that ground state is $^2A_{1u}$ rather than $^2A_{2u}$. This contrasts with the situation found for other porphyrin radical-cation species, for example, $[ZnTPP(-1)]^{\bullet+}$,[14] where the ground state has been assigned as $^2A_{2u}$. One-electron oxidation and reduction of the π ring in MgPc(-2) has been achieved chemically,[17,18] electrochemically,[17,19]

* To whom correspondence should be addressed.

(1) Stillman, M. J.; Nyokong, T. In *Phthalocyanines: Properties & Applications*; Leznoff, C. C., Lever, A. B. P., Eds.; VCH Publications: New York, 1989; pp 133-289.
(2) Nyokong, T.; Gasyna, Z.; Stillman, M. J. *Inorg. Chem.* **1987**, *26*, 1087-1095.
(3) Nyokong, T.; Gasyna, Z.; Stillman, M. J. *Inorg. Chem.* **1987**, *26*, 548-553.
(4) Ough, E.; Nyokong, T.; Creber, K. A. M.; Stillman, M. J. *Inorg. Chem.* **1988**, *27*, 2725-2732.
(5) Gouterman, M. In *The Porphyrins*; Dolphin, D., Ed.; Academic Press: New York, 1978; Vol. 3, Part A, pp 1-165.
(6) Dolphin, D.; James, B. R.; Murray, A. L.; Thornback, J. R. *Can. J. Chem.* **1980**, *58*, 1125-1132.
(7) Lever, A. B. P.; Licoccia, S.; Ramaswamy, B. S.; Kandil, S. A.; Stynes, D. *Inorg. Chim. Acta* **1981**, *51*, 169-176.
(8) Prasad, D. R.; Ferraudi, G. *Inorg. Chem.* **1982**, *21*, 4241-4245.
(9) McIntosh, A. R.; Siemiarczuk, A.; Bolton, J. R.; Stillman, M. J.; Ho, T. F.; Weedon, A. C. *J. Am. Chem. Soc.* **1983**, *105*, 7215-7223.
(10) Markovitsi; Tran-Thi, T.; Even, R. T.; Simon, J. *Chem. Phys. Lett.* **1987**, *139*, 107-112.
(11) Spikes, J. D. *Photochem. Photobiol.* **1986**, *43*, 691-699.
(12) Nevin, W. A.; Liu, W.; Melnik, M.; Lever, A. B. P. *J. Electrochem.* **1986**, *213*, 217-234.
(13) Lever, A. B. P.; Hempstead, M. R.; Leznoff, C. C.; Liu, W.; Melnik, M.; Nevin, W. A.; Seymour, P. *Pure Appl. Chem.* **1986**, *58*, 1467-1476.
(14) Browett, W. R.; Stillman, M. J. *Inorg. Chim. Acta* **1981**, *49*, 69-77.
(15) Gasyna, Z.; Browett, W. R.; Stillman, M. J. *Inorg. Chem.* **1988**, *22*, 4619-4622.
(16) Browett, W. R.; Stillman, M. J. *Biochim. Biophys. Acta* **1981**, *660*, 1-7.
(17) Clack, D. W.; Yandle, J. R. *Inorg. Chem.* **1972**, *11*, 1738-1742.
(18) Linder, R. E.; Rowlands, J. R.; Hush, N. S. *Mol. Phys.* **1971**, *21*, 417-437.
(19) Clack, D. W.; Hush, N. S.; Woolsey, I. S. *Inorg. Chim. Acta* **1976**, *19*, 129-132.

0020-1669/91/1330-2301$02.50/0

and photochemically.[20,21] Although absorption spectra of $[MgPc(-1)]^{\bullet+}$ have been previously reported,[17,18,22] there remains considerable uncertainty as to the origin of the major absorption observed between 200 and 1000 nm.[23]

In recent papers, we have utilized band deconvolution calculations to assign the electronic transitions in the absorption and the magnetic circular dichroism (MCD) spectra of phthalocyanines[2,4] and porphyrins.[24,25] In many instances, the extensive overlap of bands makes the reliable identification of band maxima and the number of bands present in the absorption spectral envelope impossible. We have found that in order to obtain reliable fitting parameters, both the MCD and the absorption spectral data must be used together.[26] The value of the MCD spectrum increases dramatically when attempts are made to assign the electronic transitions in the π-cation-radical spectra. There are simply too many transitions in many parts of the spectrum to allow the absorption spectrum to be deconvoluted without the MCD spectral data.

In this paper, we describe photochemical, electrochemical, and chemical methods used to form monomeric and dimeric $[MgPc(-1)]^{\bullet+}$ π-cation species. We report the first MCD spectra for these species and deconvolution calculations for the absorption and the MCD spectra for several $[(L)_nMgPc(-1)]^{\bullet+}$ π-cation-radical complexes.

Experimental Section

Materials and Methods. MgPc(−2) was prepared according to literature methods.[27] Imidazole (im; Fisher), sodium cyanide (Fisher), pyridine (py; BDH), 4-methylpyridine (mepy; BDH), piperidine (pip; BDH), methylimidazole (meim; Aldrich), methylene chloride (DCM; BDH), dichloroethane (DCE; BDH), and bromine (Br_2; Fisher) were used without further purification. Tetrapropylammonium perchlorate (TPAP; Kodak) was recrystallized from aqueous acetone. Carbon tetrabromide (Kodak) was recrystallized twice from 95% ethanol prior to use. The individual $(L)_2MgPc(-2)$ (L = im, CN^-, meim, py, mepy) complexes were synthesized as described previously.[4] The $[(L)_nMgPc(-1)]^{\bullet+}$ species used to provide the spectra for the deconvolution calculations, were generated by oxidation of the phthalocyanine with either 0.001 M Br_2 or 0.001 M nitric acid dissolved in DCM. This procedure was quantitative and yielded a solution with low background absorption below 250 nm.

Spectroscopic Methods. All solution spectra were recorded from nitrogen-saturated DCM and DCE solutions. Absorption spectra were recorded on a Cary Model 219 spectrophotometer. Low-temperature absorption spectra were recorded from liquid solutions cooled in an Oxford Instruments CF-204 cryostat. MCD spectra were recorded at room temperature by using a Jasco J500 C spectropolarimeter controlled by a IBM S9001 computer using the computer program CDSCAN5,[28] with a field of 5.5 T provided by an Oxford Instruments SM2 superconducting magnet. Calibration of the MCD signal intensity was performed by using an aqueous solution of cobalt(II) sulfate, with the negative band intensity at 510 nm, as $\Delta\epsilon_M = -1.9 \times 10^{-2}$ L mol^{-1} cm^{-1} T^{-1}. Electron paramagnetic resonance (EPR) spectra were recorded on a Bruker ESP 300 spectrometer. For EPR measurements, chemical oxidation using 0.001 M nitric acid in DCM was used to form the $[MgPc(-1)]^{\bullet+}$ π cation radical, the solution was then transferred to 4-mm-o.d. quartz tubes. The absolute values of the g factors were calculated from the signal of a carbon black standard.

Data Analysis. As in our previous work, Gaussian band shapes were used to fit the absorption and MCD spectra. Fitting was performed by using the program SIMPFIT,[26] which utilizes a Simplex routine, to fit the MCD spectra, and a least-squares minimization routine based on second derivatives, to fit the absorption data. The database management program Spectra Manager[29] was used to manipulate the spectral data.

Electrochemistry. The electrochemical oxidations (controlled-potential coulometry) were carried out by using Princeton Applied Research Model 273 electrochemical system controlled by an IBM instruments S9001 computer, using the computer program ELECTRA,[30] essentially as previously described.[3] Electrochemical oxidation of the MgPc(−2) complexes was carried out in DCM in the presence of 0.05 M (TPAP) using an oxidation potential of +0.7 V. All solutions were saturated with dry, deoxygenated nitrogen. For oxidations, a platinum mesh was used as the working electrode, while platinum foil was used as the auxiliary electrode. Silver wire was used as an internal standard.[3]

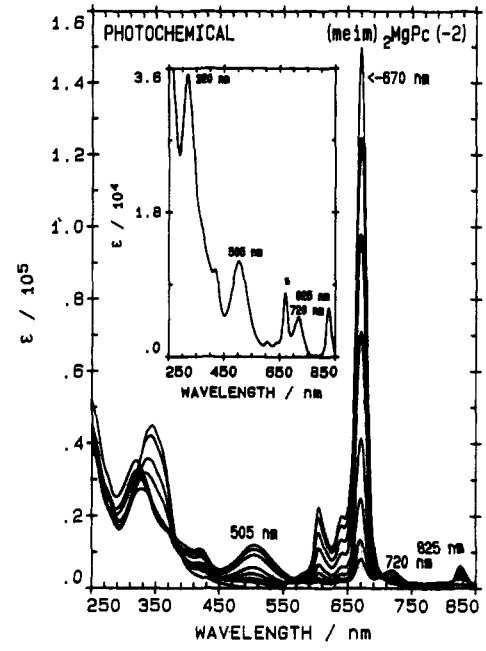

Figure 1. Absorption changes observed during the photochemical oxidation of MgPc(−2) dissolved in DCM containing 10^{-2} M CBr_4. The inset displays the absorption spectrum of the radical with less than 5% unoxidized impurity, indicated by an asterisk. The band maxima identified in Figures 1–4 were taken from the absorption spectral data.

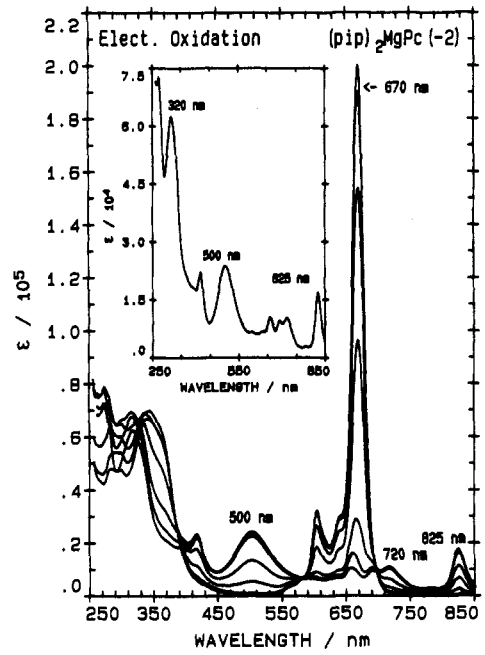

Figure 2. Absorption changes observed as controlled-potential coulometry was performed at +0.70 V vs SCE on $(pip)_2MgPc(-2)$ dissolved in DCM containing 0.05 M TPAP. The inset displays the absorption spectrum with less than 5% unoxidized $(pip)_2MgPc(-2)$.

(20) Backer, M. Jacquot, P.; Sauvage, F. X.; Vlierberge, B.; Lepoutre, G. *J. Chim. Phys.* **1987**, *84*, 429–431.
(21) Ohtani, H.; Kobayashi, T.; Ohno, T.; Kato, S.; Tanno, T.; Yamada, A. *J. Phys. Chem.* **1984**, *88*, 4431–4435.
(22) Homborg, H. *Z. Anorg. Allg. Chem.* **1983**, *507*, 35–50.
(23) Orti, E.; Bredas, J. L.; Clarisse, C. *J. Chem. Phys.* **1990**, *92*, 1228–1235.
(24) Gasyna, Z.; Browett, W. R.; Stillman, M. J. *ACS Symp. Ser.* **1986**, *321*, 298–308.
(25) Browett, W. R.; Gasyna, Z.; Stillman, M. J. *J. Am. Chem. Soc.* **1988**, *110*, 3633–3640.
(26) Browett, W. R.; Stillman, M. J. *Comput. Chem.* **1987**, *11*, 241–250.
(27) Linstead, R. P.; Lowe, A. R. *J. Chem. Soc.* **1934**, 1022–1027.
(28) Gasyna, Z.; Browett, W. R.; Nyokong, T.; Kitchenham, R. L.; Stillman, M. J. *Chemom. Intell. Lab. Syst.* **1989**, *5*, 233–246.
(29) Browett, W. R.; Stillman, M. J. *Comput. Chem.* **1987**, *11*, 73–82.
(30) Nyokong, T.; Stillman, M. J. *J. Autom. Chem.* **1986**, *8*, 122–133.

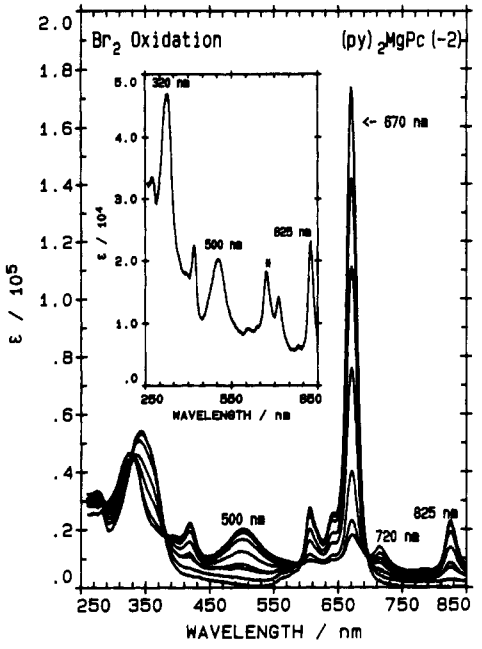

Figure 3. Absorption changes observed during the chemical oxidation of $(py)_2MgPc(-2)$ dissolved in DCM. Br_2 was used as the oxidizing agent. The inset displays the absorption spectrum of radical with less than 5% unoxidized impurity indicated by an asterisk.

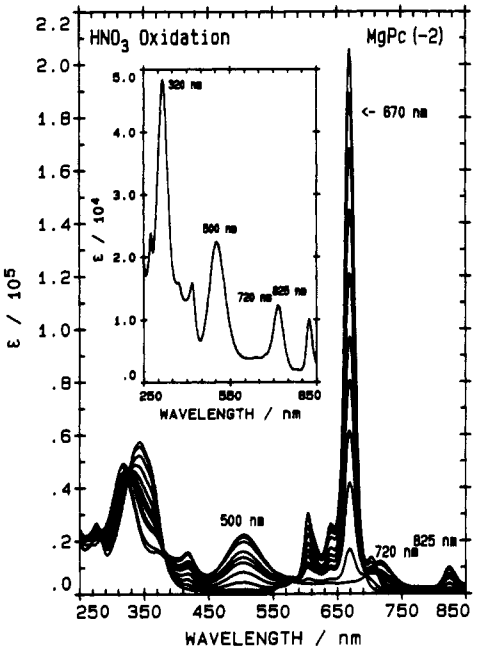

Figure 4. Absorption changes observed during the chemical oxidation of MgPc(−2) dissolved in DCM. Nitric acid dissolved in DCM was used as the oxidizing agent. The inset displays the absorption spectrum for $[MgPc(-1)]^{\bullet+}$ with no unoxidized MgPc(−2) present.

Photochemistry. For photochemical oxidations, an aliquot of the $(L)_2MgPc(-2)$ species was dissolved in nitrogen-saturated DCM made up to 0.01 M in CBr_4. The solution was irradiated with light from a 300-W tungsten–halogen Kodak projector lamp. Irradiation into the Q-band of the phthalocyanine was ensured by the use of a Corning C2 2-73 high-energy (580 nm) cutoff filter.

Results

I. Spectral Data. The oxidation of $(L)_2MgPc(-2)$ to form the radical-cation species can be readily followed in the absorption spectrum. In DCM solutions oxidation can be carried out photochemically (Figure 1), electrochemically (Figure 2), and chemically by the addition of either Br_2 (Figure 3) or nitric acid (Figure 4). In Figures 1–4, the intensities of the spectral features characteristic of the neutral MgPc(−2),[4] the Q band at 670 nm

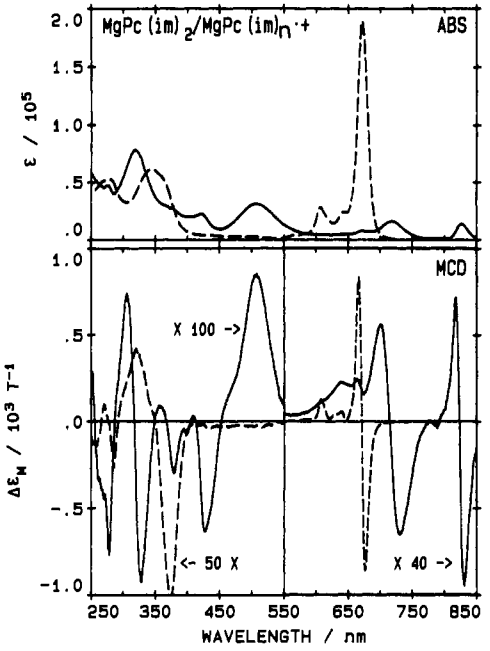

Figure 5. Absorption (ABS) and magnetic circular dichroism (MCD) spectra for neutral $(im)_2MgPc(-2)$ (dashed lines) and the one-electron oxidized $[(im)_nMgPc(-1)]^{\bullet+}$ (solid lines) recorded in DCM. Spectra were measured in 1 cm path length square UV cells or 1 cm path length cylindrical MCD cells. Note the changes in ordinate scales for the MCD traces.

and the B band at 345 nm, decrease as the oxidation proceeds. Intensities of the absorption and the MCD bands change with the axial ligand. The characteristic spectral features of phthalocyanine cation radicals at room temperature, bands centered near 825, 717, 507, and 422 nm, grow in intensity isosbestically as the oxidation proceeds with each of these methods.

Photochemical (Figure 1), electrochemical (Figure 2), and chemical oxidation using Br_2 (Figure 3), lead to incomplete oxidation of MgPc(−2). Figure 1 displays the absorption spectra obtained during photochemical oxidation of $(meim)_2MgPc(-2)$. Complete oxidation, which we associate with total loss of the 670-nm band, only takes place with considerable loss in intensity of the bands from the oxidized species. Continued irradiation in the Q-band region appears to cause disruption of the phthalocyanine ring. In Figure 1, the photolysis was stopped with about 5% of the neutral MgPc(−2) remaining.

During the electrochemical oxidation, Figure 2, new bands centered near 650 and 690 nm intensify at the end of the oxidation. The positions of these two absorption bands are those expected for the symmetry-split Q band of metal-free phthalocyanine ($H_2Pc(-2)$). With oxidation by Br_2, Figure 3, a shoulder on the low-energy side of the 670-nm band appears when oxidation exceeds 95%.

Chemical oxidation using nitric acid (Figure 4) generates the cleanest solution of $[(L)_nMgPc(-1)]^{\bullet+}$. Complete loss of the MgPc(−2) Q band at 670 nm and the retention of isosbestic points indicate that quantitative oxidation has been achieved. The inset in Figure 4 shows a spectrum of $[MgPc(-1)]^{\bullet+}$, which exhibits well-resolved bands centered on 825, 717, 507, and 319 nm. With nitric acid, the initial oxidation products are characterized by a weak absorption band near 705 nm, which grows rapidly in intensity, but later disappears as the oxidation proceeds. This band is not related by isosbestic points to the 717-nm band that is characteristic of the oxidized product. As we will discuss below, the 717-nm band arises from the dimer, $[(L)MgPc(-1)]_2^{2+}$, whereas the 825-nm band arises from monomeric $[(L)_nMgPc(-1)]^{\bullet+}$.

Figure 5 shows the room-temperature absorption and MCD spectra of $(im)_2MgPc(-2)$ and $[(im)_nMgPc(-1)]^{\bullet+}$ formed by adding Br_2 in DCM. Absorption band maxima for a range of $[(L)_nMgPc(-1)]^{\bullet+}$ π-cation-radical species are listed in Table I.

Table I. Observed Maxima in the Absorption Spectra of the Br_2-Oxidized $[(L)_nMgPc(-1)]^{\bullet+}$ species in CH_2Cl_2

$[L_nMgPc(-1)]^{\bullet+}$	λ_{max},[a] nm					
L = H_2O	826	714	506	423	320	278
L = im	827	720	507	422	319	276
L = meim	827	719	507	423	318	276
L = py	827	720	506	422	318	276
L = mepy	827	719	507	423	320	279
L = CN^-	826	718	507	416	310	
L = H_2O monomer at 300 K[b]	825	505	411	387	328	275
L = H_2O dimer at 200 K		712	510	370	317	277

[a] λ_{max} is measured directly from the absorption spectrum. See Table III for λ_{max} calculated by deconvolution of the spectral envelope. [b] Monomer spectrum recorded in 1,2-dichloroethane.

Table II. EPR Parameters for the $[(L)_nMgPc(-1)]^{\bullet+}$ Radical-Cation Species Generated Chemically (Oxidation by Br_2) in CH_2Cl_2

complex	g value	bandwidth, G
$[(H_2O)_nMgPc(-1)^{\bullet+}$	2.0039	6.75
$[(im)_nMgPc(-1)]^{\bullet+}$	2.0032	6.75
$[(meim)_nMgPc(-1)]^{\bullet+}$	2.0071	6.75
$[(py)_nMgPc(-1)^{\bullet+}$	2.0048	7.25
$[(mepy)_nMgPc(-1)]^{\bullet+}$	2.0065	5.25
$[(CN^-)_nMgPc(-1)]^{\bullet(+)-(n-)}$	2.0076	1.50

(Because of the general nature of the $(L)_n$ nomenclature, the overall charge of the π-cation-radical species will be changed if the ligand L is anionic rather than neutral.) The spectral data closely resemble the spectra obtained for π-cation-radical species of $([ZnPc(-1)]^{\bullet+})$.[3] With the loss of the intense Q bands in $[(im)_nMgPc(-1)]^{\bullet+}$ (Figure 5) three weak, but well-resolved, absorption bands appear in the window regions of the spectrum of the neutral species. These bands are centered near 825, 717, and 507 nm. The absorption band located near 507 nm is a characteristic feature of phthalocyanine π-cation-radical species and is associated with a B term in the MCD spectra, which means that the transition is to a nondegenerate state. The 825- and 717-nm bands are relatively isolated from other absorption bands and appear as A terms in the MCD spectrum, although the bandwidth of the 717-nm band (700 cm^{-1}) is considerably greater than that of the 825-nm band (200 cm^{-1}). The change in spectral properties between neutral and π cation radical is not nearly as pronounced in the B-band region as in the Q-band region. Absorption band maxima are located at 422, 319, and 276 nm for the B region of the π cation radical.

Monomeric $[MgPc(-1)]^{\bullet+}$ is difficult to obtain. However, by reducing the fraction of dimer, it is possible to construct a spectrum of the pure monomeric species. Figure 6 shows absorption and MCD spectra of monomeric $[MgPc(-1)]^{\bullet+}$ in DCE at 27 °C obtained by subtracting residual dimer bands based on the absorption at 710 nm.

The EPR signal intensity for $[MgPc(-1)]^{\bullet+}$ decreases to zero at 200 K. The room-temperature EPR g values and bandwidths (G) for the monomeric component of solutions of $[(H_2O)_nMgPc(-1)]^{\bullet+}$ and other $[(L)_nMgPc(-1)]^{\bullet+}$ species, are listed in Table II. The EPR g values calculated for the $[(L)_nMgPc(-1)]^{\bullet+}$ species are very close to the free electron value of 2.0023.

Figure 7 shows the absorption spectra of $[MgPc(-1)]^{\bullet+}$ in DCM, formed by oxidation with nitric acid, recorded between 300 and 200 K. Significant changes in band intensities are observed as the temperature falls (the inset indicates changes in absorbance as the temperature falls from 300 to 200 K). The effect is completely reversible, with recovery of the initial cation-radical spectrum when the solution is warmed to room temperature. The major changes between room temperature (300 K) and low temperature (200 K) are loss of the 825-nm band, and intensification of the 717-nm band. The absorption band intensity at 717 nm increases about 50% from 300 down to 200 K. Figure 8 shows absorption and MCD spectra of the dimeric species recorded from a solution at 200 K.

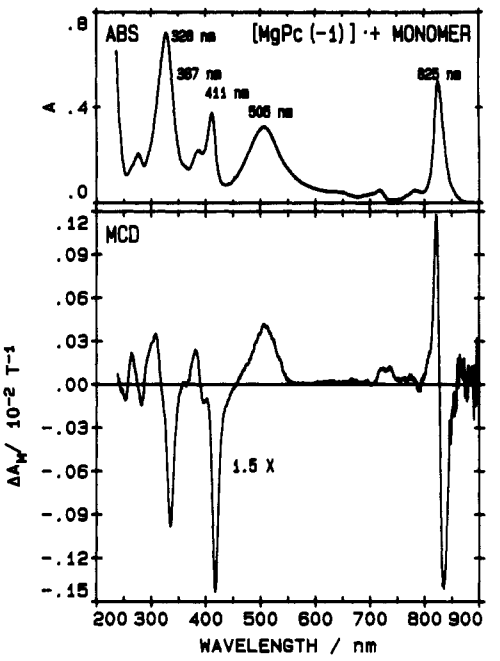

Figure 6. Absorption (ABS) and magnetic circular dichroism (MCD) spectra for monomeric $[(im)_nMgPc(-1)]^{\bullet+}$ in DCE at 300 K (spectral bands due to residual contribution by the dimer have been subtracted out).

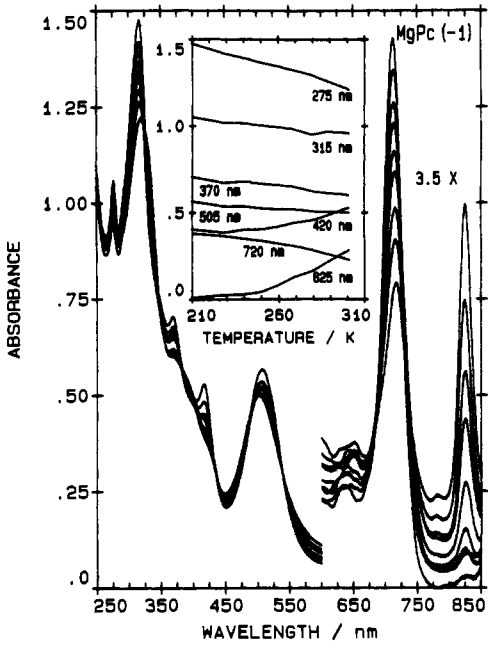

Figure 7. Absorption changes observed for $[MgPc(-1)]^{\bullet+}$ in DCM as the solution was cooled from 300 to 200 K. The inset shows intensity changes as the solution was cooled. Specifically, the band at 825 nm loses intensity, as the band at 720 nm gains intensity at 200 K. At 300 K the band at 825 nm is at maximum intensity.

II. Spectral Analysis of the Room-Temperature Spectral Data. The absorption and MCD spectral data presented in Figure 9, as the solid lines, represent the characteristic, room-temperature spectral properties of $[(L)_nMgPc(-1)]^{\bullet+}$. As with our treatment of the spectral data for ZnPc(-2),[2] $[ZnPc(-1)]^{\bullet+}$,[2] and MgPc(-2),[4] we can only identify the band positions accurately if we use band deconvolution techniques. In our analysis, we couple together the analysis of the absorption and MCD spectra in order to restrict the freedom of the minimization routines in the program. Each band has to appear in both the absorption and MCD spectrum, with the same band center and bandwidth parameters. Although several different band shapes are possible for these calculations,

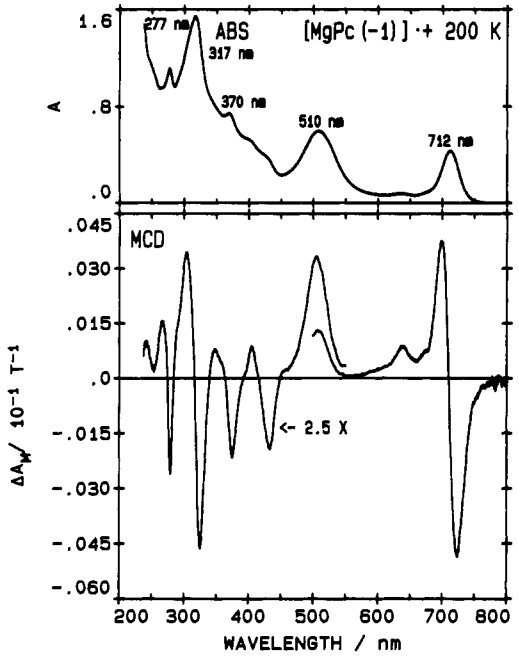

Figure 8. Absorption (ABS) and magnetic circular dichroism (MCD) spectra for dimeric $[(im)_nMgPc(-1)]^{\bullet+}$ in DCM at 200 K.

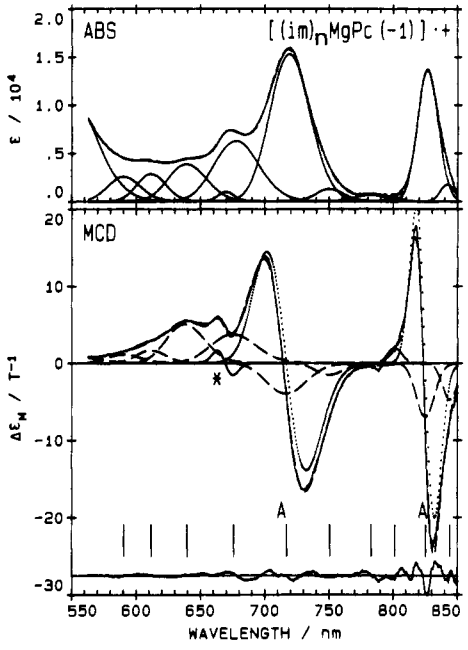

Figure 9. Results of a band analysis for $[(im)_nMgPc(-1)]^{\bullet+}$ in DCM in the visible region (bands 1–10). (a) Absorption: (—) experimental data; (- - -) fitted data; (—) individual bands. (b) MCD: (—) experimental data; (– –) fitted data; (···) A terms; (– –) B terms. The two band centers of A terms are labeled "A".

we feel that the Gaussian shape used in our calculations is satisfactory in accurately reproducing the absorption and MCD spectra for our solution data. In spite of this compromise, we believe in the reliability of the fits, since visual inspection of the absorption spectral envelopes (in Figures 9–14) shows the positioning in bands where one would expect them.

While the spectral data for $[(L)_nMgPc(-1)]^{\bullet+}$ are more complicated than the data for $(L)_2MgPc(-2)$, the Gaussian band shapes still yield reliable deconvolution results when used to fit the spectral data of the radical cation. Plotted below the MCD spectra in Figures 9–14 are the differences between the experimental and deconvoluted MCD spectra. The randomness of the noise suggests little systematic error. The greatest amount of residual noise occurs in the near-infrared region (800–870 nm) where resolution of the experimental spectra is the lowest due to a reduction of the signal to noise ratio of the spectrometer.

III. Spectral Analysis: Deconvolution of the Q-Band Region (550–850 nm). While the intense Q-band and associated A term in the MCD spectrum of MgPc(–2) are absent for $[(L)_nMgPc(-1)]^{\bullet+}$, the MCD spectrum of $[(L)_nMgPc(-1)]^{\bullet+}$ shows that degenerate states are responsible for a significant fraction of the absorption intensity in the Q-band region. In the Q region (550–850 nm) of $[(im)_nMgPc(-1)]^{\bullet+}$ (Figure 9), 6 out of the 10 fitted bands have relatively equal intensity. In the absorbance spectra, two well-resolved bands, with maxima near 825 and 717 nm, are associated with A terms in the MCD spectra (the fitting links a B term with every A term).

IV. Spectral Analysis: Deconvolution of the B-Band Region. The absorption and MCD spectra in the B-band region (250–550 nm) of $[(im)_nMgPc(-1)]^{\bullet+}$ (Figure 10) are considerably more complicated than the same region for $(im)_2MgPc(-2)$.[4] From the absorption spectra of $[(im)_nMgPc(-1)]^{\bullet+}$ (Figure 10), we observe a series of overlapping bands, several of which appear in the spectral window (400–550 nm) of the neutral phthalocyanine. Deconvolution of the absorption spectra required 18 overlapping bands to fill the envelope. This fit utilizes eight more bands than required to deconvolute the corresponding region of MgPc(–2).[4] Six of the absorption bands result from degenerate electronic transitions, since these bands corresponded to linked A and B terms in the MCD spectra. The additional 12 bands required to fill the absorption spectral envelope corresponded to B terms in the MCD spectra. Tables III and IV and Tables VI–IX (supplementary material) summarize the parameters used to fit the absorption and MCD spectra of the oxidized Q and B regions of the six $[(L)_nMgPc(-1)]^{\bullet+}$ species. Table V (supplementary material) lists band centers (nm) obtained from the deconvolution calculations for the series of $[(L)_nMgPc(-1)]^{\bullet+}$ π cation radicals analyzed in this work, where L = im, meim, py, 4-mepy, and CN^-.

V. Spectral Analysis of the Monomeric and Dimeric Absorption and MCD Data. The absorption and MCD spectral data for monomeric $[(L)_nMgPc(-1)]^{\bullet+}$, Figure 6, were analyzed in two sections, the 600–900-nm region encompassing the Q band, Figure 11, and the 200–550-nm region, which encompasses the π–π band at 505 nm and π–π^* B, N, and L bands, Figure 12. The Q-band region fits readily with a single MCD A term, followed to higher energy by a series of B terms that arise from the vibronic components in the Q_{vib} bands.

$[MgPc(-1)]^{\bullet+}$ dimerizes in many solvents at room temperature. At 200 K in DCM, the complex is completely dimerized, Figure 8. Deconvolution analysis results for the absorption and MCD spectra of the $[MgPc(-1)]^{\bullet+}$ radical cation measured at 200 K are shown in Figures 13 and 14. As is the case with other phthalocyanines,[31] we find that the 230–550-nm region does not exhibit significant marker bands for either the monomer or the dimer. The bands used in the final deconvolution calculation of the data measured at 200 K match closely many of the bands used when fitting the room-temperature data (because of temperature-dependent shifts in wavelength and absorptivity we do not expect a 1:1 match). Five A terms and a single, strong B term at 510 nm account for the most important absorption and MCD bands. As with the fits to the monomer data, the experimental and fitted lines of the absorption data superimpose, but the traces for the MCD data exhibit some errors. We do not consider the residuals to be significant.

Discussion

Oxidized metalloporphoryin species serve as vital intermediates in important biological pathways, for example, as the catalytic site in the iron-containing peroxidases and catalases.[16,25,32–34]

(31) Gasyna, Z.; Kobayashi, K.; Stillman, M. J. *J. Chem. Soc., Dalton Trans.* **1989**, 2397–2405.
(32) Gasyna, Z.; Browett, W. R.; Stillman, M. J. *Biochemistry* **1988**, *27*, 2503–2509.
(33) Browett, W. R.; Gasyna, Z.; Stillman, M. J. *Biochem. Biophys. Res. Commun.* **1983**, *112*, 515–520.
(34) Browett, W. R.; Stillman, M. J. *Biochem. Biophys. Acta* **1980**, *623*, 21–31.

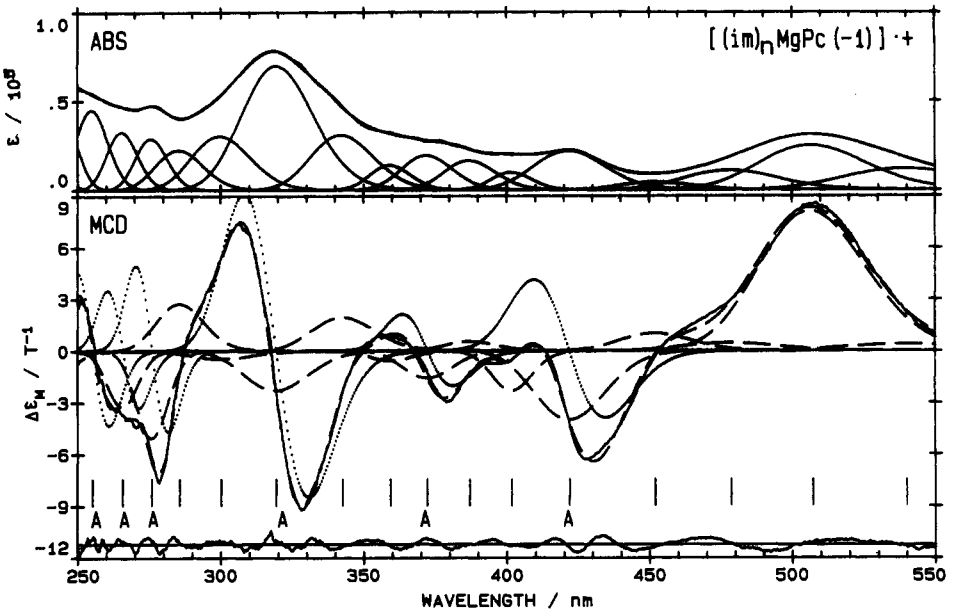

Figure 10. Results of a band analysis for $[(im)_nMgPc(-1)]^{\bullet+}$ in DCM, the ultra-violet region bands (11–27). (a) Absorption: (—) experimental data; (---) fitted data; (—) individual bands. (b) MCD: (—) experimental data; (– –) fitted data; (···) A terms; (– –) B terms. The six band centers of A terms are labeled "A".

Table III. Band-Fitting Parameters[a] for $[(im)_nMgPc(-1)]^{\bullet+}$ in CH_2Cl_2

band no.	ν, cm^{-1}	λ, nm	$\Delta\nu_f$, cm^{-1}	D_0,[b] D^2	band type	$\langle\Delta\epsilon_M\rangle_n$[c]	10^3A_1, D^2 10^3B_0,[d] D^2 cm	$(B_0/D_0)/10^{-3}$	A_1/D_0	μ,[e] μ_B
1	11848	844	188	0.089	B	−0.076	−0.50	−5.62		
2	12121	825	245	1.01	A	74.2	486.7		0.48	0.45
					B	−0.15	−0.97	−0.96		
3	12482	801	202	0.023	B	0.037	0.24	10.4		
4	12776	783	484	0.085	B	−0.010	−0.067	−0.79		
5	13326	750	451	0.14	B	−0.048	−0.31	−2.21		
6	13949	717	703	2.52	A	375.4	2462.0		0.98	0.91
					B	−0.21	−1.38	−0.55		
7	14800	676	900	1.23	B	0.24	1.60	1.30		
8	15633	640	850	0.68	B	0.30	1.97	2.90		
9	16347	612	701	0.40	B	0.091	0.60	1.50		
10	16932	591	857	0.42	B	0.064	0.42	1.00		
11	18531	540	1756	3.71	B	0.037	0.24	0.07		
12	19724	507	1702	7.05	B	0.74	4.88	0.69		
13	20907	478	1690	2.92	B	0.042	0.28	0.10		
14	22135	452	1430	0.95	B	0.071	0.46	0.48		
15	23712	422	1654	4.97	A	344.9	2261		0.45	0.42
					B	−0.30	−1.98	−0.40		
16	24905	402	1021	1.33	B	−0.10	−0.67	0.50		
17	25847	387	1400	2.93	B	0.033	0.21	0.07		
18	26879	372	1500	3.55	A	130.3	854.4		0.24	0.22
					B	−0.097	−0.64	−0.18		
19	27838	359	1294	2.13	B	−0.029	−0.19	−0.09		
20	29201	343	2200	7.59	B	0.16	1.03	0.14		
21	31337	319	2600	20.9	A	1417	9291		0.44	0.42
					B	−0.21	−1.37	−0.07		
22	33335	300	2661	7.88	B	−0.040	−0.26	−0.03		
23	35028	285	2399	5.03	B	0.20	1.31	0.26		
24	36271	276	1733	4.49	A	297.8	1953		0.43	0.41
					B	−0.26	−1.71	−0.38		
25	37658	266	1790	5.07	A	216.7	1421		0.28	0.26
					B	−0.17	−1.10	−0.22		
26	39219	255	2003	7.46	A	340.3	2232		0.30	0.28
					B	−0.009	−0.057	−0.01		
27	40663	246	1703	4.97	B	−0.047	−0.31	−0.06		

[a] Statistics. B-band region: $\lambda_{230\text{-}550\,nm}$, $\chi^2 = 0.28$, $\sum(\Delta\epsilon)^2 = 18.5$. Q-band region: $\lambda_{550\text{-}870\,nm}$, $\chi^2 = 0.51$, $\sum(\Delta\epsilon)^2 = 68.7$. [b] $D_0 = \langle\epsilon\rangle_0/326.6$, where D_0 is dipole strength; see ref 27, p 537. [c] $\langle\Delta\epsilon_M\rangle_1$ is the first moment and $\langle\Delta\epsilon_M\rangle_0$ is the zeroth moment of the MCD; when fitting with an A term, the program calculates $\langle\Delta\epsilon_M\rangle_1$, therefore $n = 1$ in the table, when fitting with a B term the program calculates $\langle\Delta\epsilon_M\rangle_0$, therefore $n = 0$ in the table. The Faraday term values, A_1 and B_0, are calculated directly from the moments as follows: $A_1 = \langle\epsilon_M\rangle_1/152.5$ and $B_0 = \langle\epsilon_M\rangle_0/152.5$. [d] See ref 27, p 537. A_1 data are printed above B_0 data when both an *A* term and *B* term are used. [e] μ = magnetic moment, calculated as $2((A_1/D_0) \times 0.4669)$. [f] All band widths are calculated as the full width at half-height.

Analysis of the optical spectral data of oxidized porphyrins and phthalocyanines has been complicated by the number of overlapping bands observed in the absorption spectra. Only recently have detailed analyses of the spectral data of oxidized porphyrins

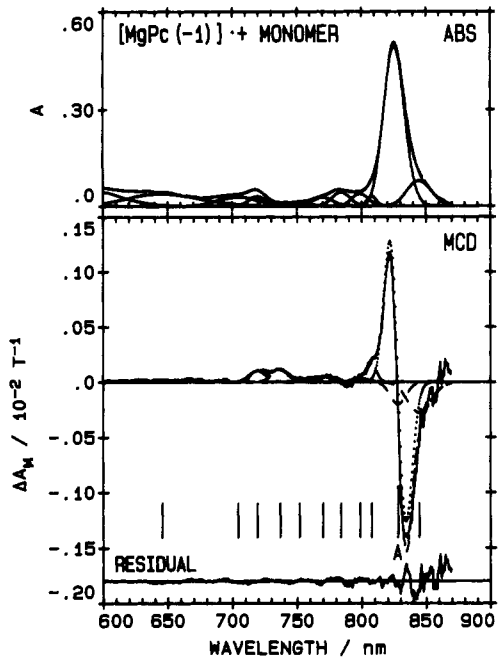

Figure 11. Results of a band analysis for the visible region of monomeric $[MgPc(-1)]^{\bullet+}$ recorded in DCE at 300 K: (—) experimental data; (---) fitted data; individual bands as in Figure 10.

Table IV. Band Centers for the Degenerate Transitions of the Monomeric and Dimeric $[(L)_nMgPc(-1)]^{\bullet+}$ Species Obtained by the Deconvolution of the Absorption and MCD Spectra

$[L_nMgPc(-1)]^{\bullet+}$ L = H_2O	band center, nm						
	Q	$\pi-\pi^a$	B_1	B_2			
dimer	717	505	422	372	319	276	255
monomer	826	509	413	387	330	315	277

[a] The nondegenerate "marker" band of oxidized phthalocyanine rings.

been reported,[15,24,35] even though the spectral properties of both tetraphenyl and octaethyl porphyrin π-cation-radical species have been known for many years.[14,36-38] The phthalocyanine spectral data for π-cation-radical species appear not to be as complicated as those for the porphyrin species, which suggests that a reasonable band assignment may be more readily achieved.

MgPc(-2) is readily oxidized and reduced, electrochemically[3,6,19,39] and photochemically.[3,20,40-42] The mechanism for the photooxidation of MgPc(-2) in the presence of an electron acceptor, with light of visible-region wavelengths, is thought to be similar to that of porphyrins such as MgOEP(-2) and MgTPP(-2). The suggested mechanism for photochemical oxidation is through the lowest lying triplet state of the phthalocyanine.[21,43]

Despite the general interest in the redox chemistry of the phthalocyanines, there have been few attempts at a quantitative assignment of the absorption spectrum. The problem in assigning these absorption spectra arises from the obvious complexity in the solution spectral data. Lack of high-quality solution spectra makes it difficult to establish the effects of variables such as solvent, axial ligand, and central metal on band energies and intensities. Published absorption spectra of ring-oxidized $[MPc(-1)]^{\bullet+}$ include the following: $[ZnPc(-1)]^{\bullet+}$,[3,21] $[RuPc(-1)]^{\bullet+}$,[6,40] $[CoPc(-1)]^{\bullet+}$,[41] $[Li_2Pc(-1)]^{\bullet+}$,[44] $[H_2Pc(-1)]^{\bullet+}$,[22] $[CuPc(-1)]^{\bullet+}$,[22] $[MgPc(-1)]^{\bullet+}$,[22] and $[FePc(-1)]^{\bullet+}$.[41] Comparison between these published $[MPc(-1)]^{\bullet+}$ spectra and the data presented here for $[MgPc(-1)]^{\bullet+}$ indicates that the spectra of $[MgPc(-1)]^{\bullet+}$ most closely resembles the spectra obtained for $[ZnPc(-1)]^{\bullet+}$ and $[RuPc(-1)]^{\bullet+}$ species, where charge-transfer bands do not lie in the same region. However, a major contributor to the spectral complexity is the presence of both monomers and dimers at room temperatures.

I. Oxidation of Magnesium Phthalocyanine. Chemical oxidation using nitric acid is the cleanest method to form $[(L)_nMgPc(-1)]^{\bullet+}$. With photochemical oxidation, there appears to be bleaching of the oxidized complex as oxidation approaches completion. Electrochemical oxidation appears to generate a small amount of metal-free phthalocyanine, while chemical oxidation using Br_2 either generates a small amount of metal-free phthalocyanine or because of bromine's strong oxidizing power ($E_{1/2}$ = 1.09 V versus SCE in aqueous solutions), causes some of the π cation radical to be further oxidized to the dication.

A transient species is encountered during the chemical oxidation of MgPc(-2) with nitric acid (Figure 4). At the onset of the reaction an additional band at 705 nm appeared, intensified, and then disappeared as the oxidation reached completion. One possible explanation for this band is the formation of the mixed $[(L)MgPc(-2)(L)MgPc(-1)]^{\bullet+}$ dimeric species, with subsequent formation of the cation radical. As the oxidation proceeds toward completion, excess nitric acid quantitatively forms the radical, with loss of the 705-nm absorption band.

II. Variable-Temperature Absorption and EPR Spectra of $[MgPc(-1)]^{\bullet+}$. Our results indicate that ring-oxidized magnesium phthalocyanine exists as a mixture of monomeric and dimeric π-cation-radical species at room temperature. Homborg[22] has suggested that the π cation radical readily dimerizes in polar solvents existing mainly as the dicationic $[MgPc(-1)]_2^{2+}$ species, while in nonpolar solvents the monomeric $[MgPc(-1)]^{\bullet+}$ species predominates. The presence of the two marker bands in the room-temperature absorption spectra for $[(L)_nMgPc(-1)]^{\bullet+}$ in DCM shows that a mixture of monomer and dimer exists. The variable temperature absorption (Figure 7) and EPR spectra of $[MgPc(-1)]^{\bullet+}$ confirm this conclusion.

We assign the 825-nm band to monomeric $[MgPc(-1)]^{\bullet+}$ while the 720-nm band is assigned to the dimeric $[MgPc(-1)]_2^{2+}$ species. The assignment of the 825- and 717-nm bands is consistent with previous studies of phthalocyanines, which indicate a blue shifting of the Q absorption band upon dimerization.[1,31]

III. Band Assignments. The Q, B, N, L, and C labels were commonly used to describe the major bands in the absorption spectra of porphyrins and phthalocyanines by Gouterman's group.[5,45,46] For the porphyrins, there seems to be no ambiguity between the early absorption data and spectra measured more recently: the assignments are consistent for spectra measured in the vapor, solution, and solid phases. For the metallophthalocyanines, we have long believed that two major bands lie in the 300-380-nm region. It was clear from the spectra of $Li_2Pc(-2)$[47] with added CN^- ligand that the absorption envelope in the 350-nm region arose from two degenerate transitions. Band deconvolutions for ZnPc(-2)[2] and for MgPc(-2)[4] confirmed this observation. In the Nyokong, Gasyna, and Stillman[2] and Ough, Nyokong, Creber, and Stillman[4] papers, we adjusted the Gouterman order such that the second 350-nm band became the N band. In earlier work on α-phase sublimed films, we had assigned a second band under the "B" envelope as B2. This assignment was based on the work of Henriksson and Sundboom.[48,49] In the Gouterman[45] and Hen-

(35) Gasyna, Z.; Stillman, M. J. *Inorg. Chem.* **1990**, *29*, 5101-5109.
(36) Gasyna, Z.; Browett, W. R.; Stillman, M. J. *Inorg. Chem.* **1984**, *23*, 382-384.
(37) Gasyna, Z.; Browett, W. R.; Stillman, M. J. *Inorg. Chem.* **1985**, *24*, 2440-2447.
(38) Dolphin, D. *Isr. J. Chem.* **1981**, *21*, 67-71.
(39) Jones, J. G.; Twigg, M. V. *Inorg. Nucl. Chem. Lett.* **1970**, *6*, 245-247.
(40) Nyokong, T.; Gasyna, Z.; Stillman, M. J. *Inorg. Chim. Acta* **1986**, *112*, 11-15.
(41) Nyokong, T.; Gasyna, Z.; Stillman, M. J. *ACS Symp. Ser.* **1986**, *321*, 309-327.
(42) Van Vlierberge, B.; Ferraudi, G. *Inorg. Chem.* **1987**, *26*, 337-340.
(43) Ferraudi, G. J.; Prasad, D. R. *J. Chem. Soc., Dalton Trans.* **1980**, 2137-2140.
(44) Homborg, H.; Kalz, W. *Z. Naturforsch.* **1978**, *33B*, 1067-1071.
(45) Edwards, L.; Gouterman, M. *J. Mol. Spec.* **1970**, *33*, 292-310.
(46) Gasyna, Z.; Browett, W. R.; Stillman, M. J. *ACS Symp. Ser.* **1986**, *321*, 298-308.
(47) Stillman, M. J.; Thomson, A. J. *J. Chem. Soc., Faraday Trans.* **1974**, *70*, 805-814.
(48) Henriksson, A.; Roos, B.; Sundbom, M. *Theor. Chim. Acta* **1972**, *27*, 303-313.

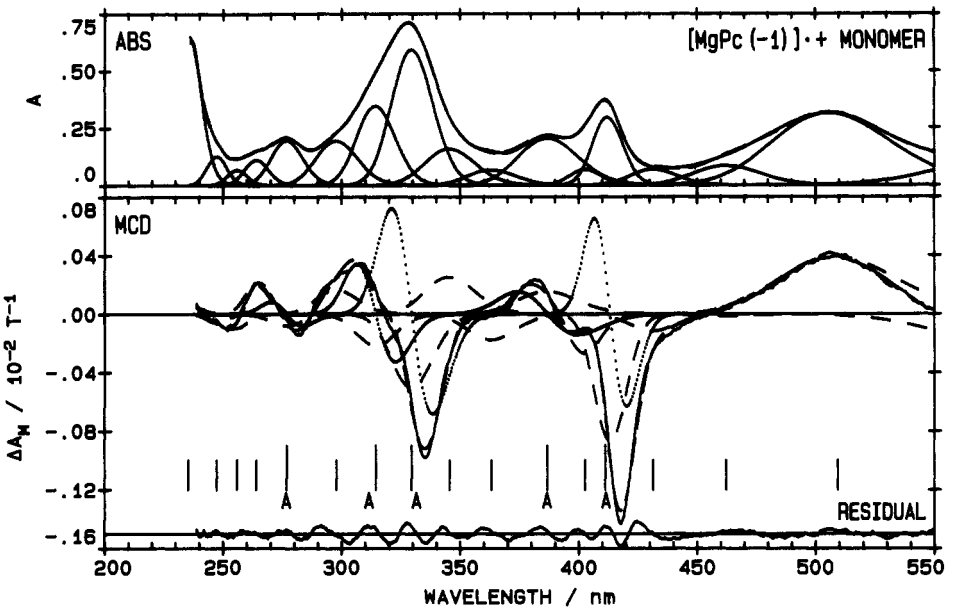

Figure 12. Results of a band analysis for the ultraviolet region of monomeric $[MgPc(-1)]^{\bullet+}$ absorption spectra, recorded in DCE at 300 K: (—) experimental data; (--) fitted data; individual bands as in Figure 10.

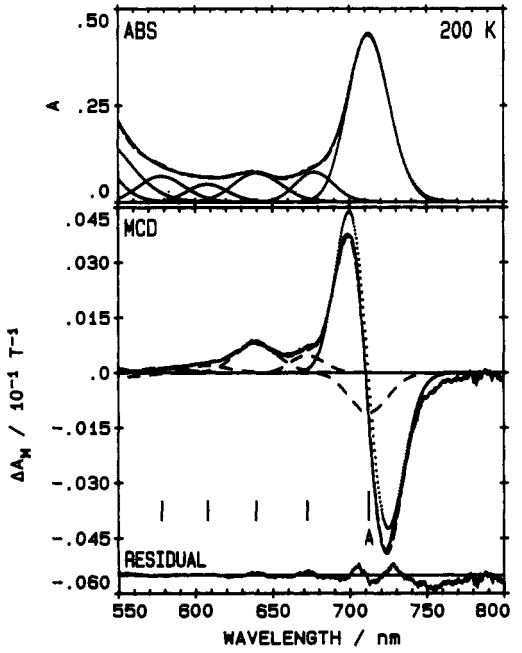

Figure 13. Results of a band analysis for the visible region of dimeric $[MgPc(-1)]^{\bullet+}$ recorded in DCM at 200 K: (—) experimental data; (---) fitted data; individual bands as in Figure 10.

riksson and Sundboom[48,49] calculations, the MO origins of the B state are listed as a combination of several transitions. Although two B bands are not listed in a recent Xα calculation by El Khatib et al.[50] for ZnPc(−2), the data for allowed transitions (Table VI in ref 50) lists additional unassigned transitions in the 30000-cm^{-1} region. With this in mind, we concur with Van Cott et al.[51] and now return to our earlier labeling of Q, B1, B2, N, L, and C for the set of bands observed in the neutral species between 800 and 220 nm.

The preceeding discussion is related directly to the assignment problem in the π-cation-radical species. We need to decide on the total number of transitions in the neutral complex before we can identify new π−π transitions, in the spectrum of the radical. As above, analysis of the spectral data of both $[ZnPc(-1)]^{\bullet+}$ and $[(L)_nMgPc(-1)]^{\bullet+}$ is an essential step toward solving the assignment problem because of the absence of any metal-related transitions. Figure 15 displays the molecular orbitals that give rise to states in the energy region 10000–50000 cm^{-1}. Selection rules for D_{4h} restrict us to transitions from $^2A_{1u} \rightarrow {}^2E_g$ and $^2A_{1u} \rightarrow {}^2A_{2g}$. The former will result in MCD A and B terms, the latter in just B terms. We expect orbital transitions from the half-filled a_{1u} level into empty e_g level(s) and into the half-filled a_{1u} molecular from low-lying molecular orbitals.

IV. Comparison between Bands Obtained from the Deconvolution Calculations and Bands Predicted by Theoretical Calculations. Although theoretical calculations of band energies for a variety of neutral metallophthalocyanines and porphyrins are available and have been compared with experimental calculations for many years, it is only recently that attempts have been made to interpret the absorption spectra of the oxidized π-cation-radical species. Minor et al.[52] reported a theoretical interpretation of data they recorded for cationic and anionic absorption spectra of a variety of MPc(−2)'s. The band assignments of Minor et al.[52] are complicated by the fact that many of the spectra were obtained from samples in the solid state, in which intermolecular effects, such as Davydov coupling, broaden, shift, and duplicate many of the bands.[53]

The removal of an electron from the highest filled orbital of MgPc(−2) does not change the orbital degeneracy of the ground or excited state. In the absorption and MCD spectra we still expect the five ring-based degenerate π−π* electronic transitions assigned as the Q, B1, B2, N, and L bands. A terms are expected in the MCD spectra, since the electronic transitions are from the $^2A_{1u}$ ground state into an ^2E_g excited state. In addition, transitions into the half-filled HOMO (a_{1u}) level may also give rise to MCD A or B terms depending on the degeneracy of the lower level. These new transitions can extend from the near-infrared (900 nm) to the spectral window (400–550 nm) region of the neutral MgPc(−2).

Band maxima, measured directly from absorption spectra, of various $[(L)_nMgPc(-1)]^{\bullet+}$ species (Table I) are useful in the identification of $[MPc(-1)]^{\bullet+}$ spectra, but because of the complexity of the spectral envelope and in particular the presence of both monomers and dimers, these data are of little use in the

(49) Henriksson, A.; Sundbom, M. *Theor. Chim. Acta* **1972**, *27*, 213–222.
(50) El Khatib, N.; Boudjema, B.; Maitrot, M.; Chermette, H.; Porte, L. *Can. J. Chem.* **1988**, *66*, 2313–2324.
(51) Van Cott, T. C.; Rose, J. L.; Misener, G. C.; Williamson, B. E.; Schrimp, A. E.; Boyle, M. E.; Schatz, P. N. *J. Phys. Chem.* **1989**, *93*, 2999–3005.
(52) Minor, P. C.; Gouterman, M.; Lever, A. B. P. *Inorg. Chem.* **1985**, *24*, 1894–1900.
(53) Hollebone, B. R.; Stillman, M. J. *Chem. Phys. Lett.* **1974**, *29*, 284–286.

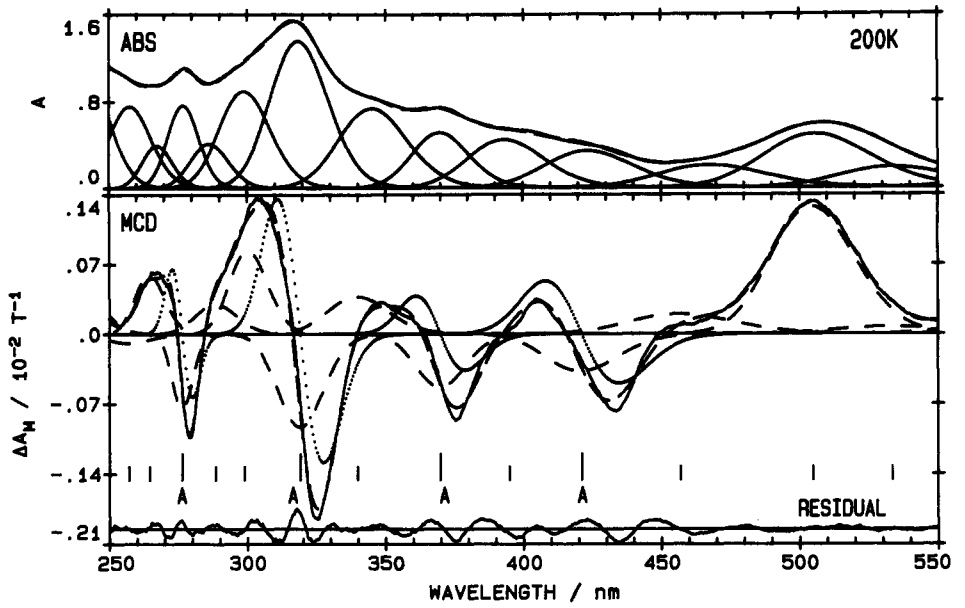

Figure 14. Results of a band analysis for the ultraviolet region of dimeric $[MgPc(-1)]^{\bullet+}$ absorption spectra, recorded in DCM at 200 K: (—) experimental data; (---) fitted data; individual bands as in Figure 10.

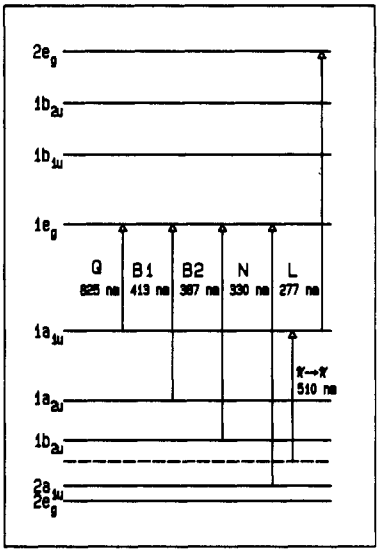

Figure 15. Selected molecular orbitals of the radical cation phthalocyanines. The band wavelengths are taken from the deconvolution calculations of the monomer data shown in Figures 12 and 13. The order of the orbitals has been adapted from ref 5.

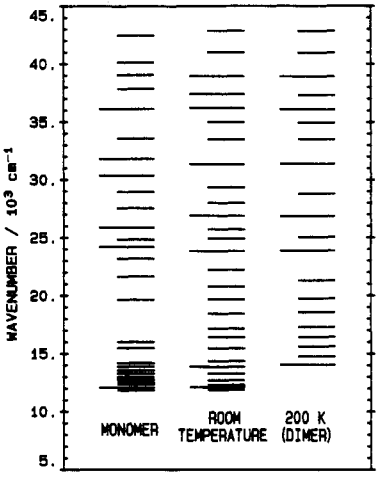

Figure 16. Comparison between the energies of bands in the spectra of monomer, dimer, and the room-temperature mixture of monomer and dimer for $[(im)_nMgPc(-1)]^{\bullet+}$, calculated by band deconvolution of the absorption and MCD spectra.

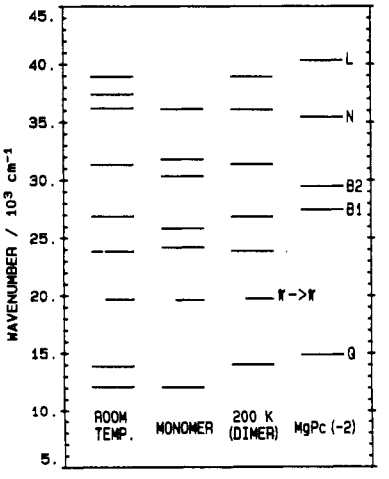

Figure 17. Comparison between the energies of degenerate states in $[MgPc(-1)]^{\bullet+}$ and MgPc(−2), calculated by deconvolution of the monomeric and dimeric spectral data, compared with the assignment reported for the neutral MgPc(−2).[4]

assignment of band energies. Deconvolution of the Q (Figure 9) and B (Figure 10) regions of $[(im)_nMgPc(-1)]^{\bullet+}$ shows that band centers are not always positioned at the absorption maxima and that several transitions can overlap to give rise to an absorption band.

V. Deconvoluted Results for Monomeric and Dimeric $[MgPc(-1)]^{\bullet+}$. The difference in energy between the Q band in the oxidized monomeric and dimeric $[MgPc(-1)]^{\bullet+}$ can be used to estimate the energies of the B1, B2, N, and L bands from the spectral data. The deconvolution results obtained for the absorption and MCD spectra of monomeric, dimeric, and room-temperature solutions of $[MgPc(-1)]^{\bullet+}$ are shown in Figure 16. Using the assignments proposed in Figure 15, we can compare the composition of the spectral envelope of $MgPc(-2)$[4] with that of $[MgPc(-1)]^{\bullet+}$ (Figure 17). Clearly, the degenerate bands at 372, 319, 276, and 255 nm in the monomer line up closely enough with the B1, B2, N, and L bands of the neutral species for us to suggest that these bands are those of the oxidized species. Adopting this assignment implies that oxidation of the phthalocyanine ring reorganizes the molecular orbitals such that the energy difference between the ground state and excited state is reduced and a red shift is observed. In a recent valence effective Hamiltonian calculation for $[LiPc(-1)]^{\bullet+}$, Orti et al.[23] predicted

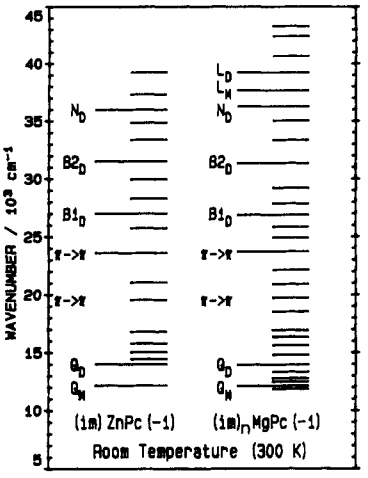

Figure 18. Comparison between the energy levels of $[(im)_nMgPc(-1)]^{\bullet+}$ and $[(im)ZnPc(-1)]^{\bullet+}$ calculated by band deconvolution of the absorption and MCD spectra of these two complexes (data for $[(im)ZnPc(-1)]^{\bullet+}$ replotted from ref 2.

the energies and polarizations of transitions between 800 and 306 nm. Transitions polarized x,y are predicted at 317, 316, 311, and 306 nm. It is not easy to associate any one of these with a specific band in the experimental spectra because the energy range is so small when compared with the range observed (370–255 nm). Their prediction of the $2a_{1u}$–$6e_g^*$ Q transition at 764 nm is very close to the observed value of 825 nm.

VI. Assignment of the 507-nm Band of $[MgPc(-1)]^{\bullet+}$. The MCD B term centered near 507 nm in both the monomer and the dimer is relatively isolated from other bands being located in the "window region" of many neutral phthalocyanines. This band is one of the most intense in the absorption spectrum, and it is often used as a "fingerprint" marker for formation of the π cation radical.[3,41,52] While it has been suggested that this band has π–π^* origins, possibly the displaced Q band,[1,22,52] the nondegenerate nature of the transition strongly suggests that it is neither the Q band nor the B1 band but a low-lying π–π transition. Because a similar band is observed for each of the $[MPc(-1)]^{\bullet+}$ species we have studied previously,[3,6] we conclude that the band does not arise from axial ligand to phthalocyanine ring charge transfer or from any metal-related transitions. In the Orti et al.[23] calculation for $[LiPc(-1)]^{\bullet+}$, it is predicted that bands near 411 and 512 nm are π–π in character. However, this proposed assignment requires x,y degeneracy for the 512-nm transition. Clearly, this important band in the radical-cation spectrum of both monomers and dimers is nondegenerate.

VII. Comparison between the Deconvolution Data for $[(im)_nMgPc(-1)]^{\bullet+}$ and $[(im)ZnPc(-1)]^{\bullet+}$. While the deconvolution calculations are very complicated, the plots of the residuals for the MCD spectra (Figures 9–14) do indicated the accuracy of the fits; however, reproduction in a series of spectra for related complexes enhances the reliability of the calculations. Figure 18 compares the results of independent calculations from spectra measured at room temperature for $[(im)_nMgPc(-1)]^{\bullet+}$ with those obtained for $[(im)ZnPc(-1)]^{\bullet+}$.[2] It is apparent that the major calculated bands are at the same energies in both species. Figure 18 shows that $[(im)_nMgPc(-1)]^{\bullet+}$ required many more bands to completely fit the spectral envelopes (Figures 9 and 10) than were required for $[(im)ZnPc(-1)]^{\bullet+}$. These additional bands are the result of better spectral resolution in the near-infrared region and extended range into the ultraviolet region.

A discrepancy in band types required for deconvolution occurs in the two bands that arise at slightly higher energy than the C band. For $[(im)_nMgPc(-1)]^{\bullet+}$, the best fit used linked MCD A and B terms, which indicates degenerate transitions in contrast to our findings for $[(im)ZnPc(-1)]^{\bullet+}$ where nondegenerate transitions were suggested. Since the $[(im)_nMgPc(-1)]^{\bullet+}$ spectra extend farther into the ultraviolet region, it appears that the enhanced range between 35 000 and 41 000 cm^{-1} has isolated these two additional degenerate electronic transitions.

Conclusions

Absorption and EPR spectra recorded for oxidized $[MgPc(-1)]^{\bullet+}$, at various temperatures, indicate that the room-temperature solution consists of a mixture of monomer and dimer. For $[(im)_nMgPc(-1)]^{\bullet+}$, five degenerate transitions are centered near 717, 372, 319, 276, and 255 nm and are assigned from low to high energy as the Q, B1, B2, N, and L bands of the dimeric $[MgPc(-1)]_2^{2+}$ species. In room-temperature solutions, bands are also observed at 825 and 266 nm, which are assigned as the Q and L bands of monomeric $[(L)_nMgPc(-1)]^{\bullet+}$. The nondegenerate 507-nm band is assigned as a π–π transition. Deconvolution analysis of the spectral data for the pure monomeric and dimeric species yields band centers of transitions to degenerate states at 826 (Q), 413 (B1), 387 (B2), 330, 315, and 277 nm for the monomer and 717 (Q), 422 (B1), 372 (B2), 319, 276, and 255 nm for the dimer. The MCD data allow unambiguous assignment of the Q band for both monomeric and dimeric species.

Acknowledgment. We wish to acknowledge and thank Dr. Tebello Nyokong, currently at the Department of Chemistry, National University of Lesotho, for the preliminary work carried out on this project. We thank the NSERC of Canada for operating and equipment grants, and Imperial Oil, Ltd., Canada, for financial support. The Bruker EPR spectrometer was purchased with grants from the NSERC of Canada and the Academic Development Fund at the UWO (to J. R. Bolton, M. J. Stillman, and S. K. Wong). We are associated with the Centre for Chemical Physics and the Photochemical Unit at the UWO. This is Publication No. 435 of the Photochemical Unit.

Supplementary Material Available: Five additional tables of band-fitting parameters (Tables V–IX) that were calculated for each of the $[(L)_nMgPc(-1)]^{\bullet+}$ complexes discussed in this study (10 pages). Ordering information is given on any current masthead page.